# N-Terminal Domain of *Avena* Phytochrome: Interactions with Sodium Dodecyl Sulfate Micelles and N-Terminal Chain Truncated Phytochrome†

William Parker,‡ Mick Partis,§ and Pill-Soon Song*,‡

*Department of Chemistry and Institute for Cellular and Molecular Photobiology, University of Nebraska, Lincoln, Nebraska 68588, and Institute of Horticultural Research, Littlehampton, West Sussex BN17 6LP, U.K.*

*Received May 13, 1992; Revised Manuscript Received July 16, 1992*

ABSTRACT: Phytochrome is the ubiquitous red light photoreceptor present in plants. Properties of the 6-kDa end terminal region of phytochrome A (PHYA from etiolated *Avena*) have been investigated by the use of synthetic polypeptide fragments corresponding to that region. This region of the phytochrome A protein has been viewed as a possible functional site due to the large differences in the sequence's conformation and exposure between the Pr (red light-absorbing form) and Pfr (far-red light-absorbing, gene-regulating form) species of phytochrome A. Hydrophobic moment calculations reveal amphiphilic helical potential in this section of the protein, consistent with the folding of the N-terminal region onto a hydrophobic chromophore/chromophore pocket. A large N-terminal synthetic peptide also demonstrated helical folding in the presence of SDS micelles. This experimental evidence indicates that the N-terminal $\alpha$-helical folding upon conversion of the regulatorily inactive Pr to the active Pfr form of phytochrome A is likely driven at least in part by amphiphilic helix stabilization. Further, the large synthetic peptide was spectrally demonstrated to interact with phytochrome A lacking the N-terminal region. The formation of this nativelike complex may provide us with a tool for both biophysical and physiological studies on the mechanism of phytochrome A signal transduction.

Phytochrome A, or dark-grown phytochrome, is the most well-characterized photosensor protein present in plants. This protein is present in two conformationally and spectrally distinct forms. The far-red-absorbing form (Pfr) and the red absorbing form (Pr) of phytochrome A undergo the reversible photoconversions which are responsible for a wide variety of plant regulatory and morphological processes as follows:

$$\mathrm{Pr} \underset{730\ \mathrm{nm}}{\overset{666\ \mathrm{nm}}{\rightleftharpoons}} \mathrm{Pfr} \rightarrow \text{multiple plant responses}$$

A considerable amount of study concerning phytochrome A has centered around the first 50–70 amino acids of the 124-kDa *Avena* chromoprotein (PHYA). This N-terminal segment has several properties which distinguish it from the rest of the peptide chain. For a number of years, phytochrome A was routinely isolated and studied in a partially degraded or "large" form. This 114–118-kDa form primarily resulted from truncation of an approximately 6-kDa region from the N-terminus by proteolytic cleavage during isolation (Vierstra & Quail, 1983a). Later isolation of intact phytochrome A has revealed distinct spectral differences between large (114–118 kDa) and intact (124 kDa) phytochrome A (Vierstra & Quail, 1983a,b).

Interestingly, intact Pr and Pfr showed a difference in helical content as measured by circular dichroism (CD) while large phytochrome A did not (Vierstra et al., 1987). A 7–23% increase in ellipticity at 222 nm is seen by CD upon Pr to Pfr photoconversion. [The difference is dependent on the type of buffer used (Sommer & Song, 1990).] This apparently corresponds to a 3–5% increase in $\alpha$-helix and involves 37–56 residues (out of 1128 residues) as intact phytochrome A is converted from Pr to Pfr [Sommer and Song (1990); unpublished data on *Pisum* phytochrome A by L. Deforce, S. Tokutomi, and P.-S. Song, (1992)]. Monoclonal antibody binding at the N-terminal region of intact phytochrome A abolished the change in CD signal (Chai et al., 1987a). These results indicate that the N-terminal segment of phytochrome A is involved in photoreversible $\alpha$-helical folding upon Pr to Pfr phototransformation. Further, since no CD change is seen in large phytochrome A or anti-N-terminal antibody treated phytochrome A, it is likely that the only change in secondary structure is localized within the 6-kDa N-terminal region of 124-kDa phytochrome A (Chai et al., 1987a).

Proteolytic cleavage patterns (Jones et al., 1985), phosphorylation sites (Wong et al., 1986), and differential antibody binding (Cordonnier et al., 1985) of Pr vs Pfr phytochrome A indicate that the N-terminus of intact phytochrome A undergoes a significant conformational and/or topographic change upon photoconversion. These studies demonstrate that the N-terminus is considerably more exposed to proteolytic and enzymatic action as well as antibody binding in the Pr form.

The N-terminal domain of phytochrome A is considered a likely candidate for a functional role in signal transduction due to the unique conformational/topographical changes of that region. Further study of the phytochrome A protein including this very unique N-terminal segment is an important and necessary step in the elucidation of the as yet unknown signal transduction mechanism of phytochrome A. Even the receptor(s) is (are) unknown. In order to further characterize the $\alpha$-helical folding of the phytochrome A N-terminus, we have studied the properties of synthetic N-terminal fragments of *Avena* phytochrome A as well as the interaction between these fragments and phytochrome A. Particular attention has been paid to the possibility of amphiphilic $\alpha$-helical folding of this region, a common receptor/effector motif in mammalian systems.

Recently, Cherry et al. (1991, 1992) demonstrated that a large phytochrome A mutant (missing residues 7–69) trans-

† This work was supported by USPHS NIH Grant GM36956.
* To whom correspondence should be addressed.
‡ University of Nebraska.
§ Institute of Horticultural Research.

0006-2960/92/0431-9413$03.00/0 

genically expressed in tobacco had no physiological activity, while wild-type protein produced typical phytochrome A mediated responses under the same conditions. This mutant (large) phytochrome A lacked biological activity even though it was expressed and stable at the same levels as wild type, incorporated chromophore, and was photoreversible (Cherry et al., 1991, 1992). This is suggestive evidence that the N-terminus of phytochrome A is necessary for correct receptor binding, although direct docking between a receptor and the N-terminus has yet to be demonstrated.

In this study, we have examined the far N-terminal 6-kDa sequence of phytochrome A for the presence of amphiphilic helix potential using the calculation method of Eisenberg et al. (1982). We have also synthesized peptides corresponding to this N-terminal region and have analyzed the helix-forming ability of these peptides in an amphiphilic environment [sodium dodecyl sulfate (SDS) micelles]. SDS micelles are known to induce $\alpha$-helix in amphiphilic peptides, while this is not the case for nonamphiphilic peptides (Lark et al., 1989; Pasta et al., 1990; Tsikaris et al., 1989; Wu & Yang, 1981). Other detergents forming amphiphilic micelles apparently have a similar effect on amphiphilic peptides (Lauterwein et al., 1979). We have also begun initial study of the interaction of these peptides with phytochrome A, which lacks a covalently linked N-terminal region.

## MATERIALS AND METHODS

*Peptide Synthesis.* Peptide synthesis of the first 54 residues of *Avena* phytochrome A was carried out on a Vega Coupler 2200 peptide synthesizer using 0.5-mmol-scale Fmoc chemistry. An N-terminal methionine is posttranslationally cleaved from the protein in vivo and is not counted in the peptide sequence. The sequence is as follows: *N*-acetyl-Ser-1, Ser-2, Ser-3, Arg-4, Pro-5, Ala-6, Ser-7, Ser-8, Ser-9, Ser-10, Ser-11, Arg-12, Asn-13, Arg-14, Gln-15, Ser-16, Ser-17, Gln-18, Ala-19, Arg-20, Val-21, Leu-22, Ala-23, Gln-24, Thr-25, Thr-26, Leu-27, Asp-28, Ala-29, Glu-30, Leu-31, Asn-32, Ala-33, Glu-34, Tyr-35, Glu-36, Glu-37, Ser-38, Gly-39, Asp-40, Ser-41, Phe-42, Asp-43, Tyr-44, Ser-45, Lys-46, Leu-47, Val-48, Glu-49, Ala-50, Gln-51, Arg-52, Asp-53, Gly-54-amide. A 0.46 mmol/g substituted amide resin was used for synthesis. By amino acid analysis of small peptides synthesized on the amide resin, we determined that roughly 50% of functional sites were lost between the first and second coupling reactions. This, in effect, produced a sparsely substituted resin (less than 0.25 mmol/g), which is necessary for synthesis of large peptides. All coupling reactions were monitored by a ninhydrin test, and synthesis was only continued if no reaction with ninhydrin was observed (greater than 99% complete coupling). Using this criterion, more than 50% of all peptide couplings were repeated (double coupling). All free N-terminal amines which remained after coupling were blocked (using acetic anhydride) to prevent further reaction. After cleavage from the resin using trifluoroacetic acid and suitable scavengers, the peptide was dried and hydrophobic impurities were partially removed by diethyl ether extraction. Approximately 500 mL of 10% acetic acid in $H_2O$ was then used to resolubilize the peptide; 100-mL aliquots of this aqueous phase were extracted twice with 50-mL portions of ethyl acetate/ether (2:1). Upon addition of 50 mL of dichloromethane to the aqueous peptide solution, the peptide was incorporated into a stable emulsion phase between the organic and aqueous phases. Emulsified samples allowed to stand more than 6 months have shown no change. The peptide emulsion was dried and the extraction procedure was repeated, again resulting in a peptide emulsified in $H_2O$/dichloromethane. The peptide was then separated from lower molecular weight contaminants by Biogel P6 (fine grade) chromatography in 67% acetic acid. Amino acid analysis of the peptide after chromatography yielded expected results except that the proline and serine quantities indicated some truncation had occurred during synthesis very close to the N-terminus (within five or six residues) in approximately 20% of the peptide. Thus, approximately 80% (molar) of the peptide is present as a 54-mer with the remaining 20% present as slightly lower molecular weight peptides. Amino acid analysis and sequencing were carried out on peptides obtained by HPLC purification of a tryptic digest of the 54-mer in order to verify complete synthesis. This approach was successful, except that the far N-terminal fragment (Ac-SSSRPASSSSSR) was not isolated. However, the amino acid analysis of the entire peptide does indicate that the far N-terminal five or six residues (containing the only proline in the sequence) were successfully coupled to the peptide. Mass spectrometry on the intact peptide was unsuccessful. (There was no signal above the noise level.) This was likely due to the poor solubility of the peptide, even though a number of solvents were investigated. The Biogel P6 purified peptide was lyophilized and used in all subsequent experiments by dissolving the dry peptide in the appropriate buffer.

The peptides SSSRPASSSSSRNRQSSQ and VSRNLLRLMNGDVRHC correspond to residues 1–18 and 1090–1104 of oat phytochrome A, respectively. The cysteine residue at the C-terminus of the 1090–1104 peptide was attached for use in other experiments not described here. Both of these peptides were synthesized on a Biosearch Model 9500 apparatus using standard solid-phase t-Boc chemistry. Peptides were cleaved from the resin with HF and contaminating low molecular weight material was removed by chromatography on Biogel P2 in 67% acetic acid. The fidelity of synthesis was checked by sequencing on an Applied Biosystems 470A apparatus.

*Chemicals and Reagents.* Sodium dodecyl sulfate (SDS) was purchased from Bio-Rad Laboratories, Richmond, CA. Glycerol, type I peptone from meat (16% total nitrogen, 3% amino nitrogen), and sodium phosphate were obtained from Sigma Chemical Co., St. Louis, MO. Fmoc amino acids, solvents, and other reagents for synthesis of the 54-mer were purchased from Vega Biotechnologies, Tucson, AZ. All reagents were peptide synthesis grade purity. RapidAmide resin for synthesis of C-terminal amide peptides were purchased from NEN Research Products, Boston, MA. Deionized water further purified by a Barnstead Nanopure ultrapure water system or by filtration and distillation was used for all experiments. Intact phytochrome A (the purity index or SAR = 0.9–1.05) was isolated by a modification of the Vierstra and Quail (1983a) and Chai et al. (1987b) methods as previously described (Sommer & Song, 1990). Large phytochrome A was isolated by a similar method, except that the protease inhibitor phenylmethanesulfonyl fluoride was not used and the phytochrome A was kept in the Pr form until application to hydroxyapatite chromatography. The intact phytochrome A used had a Pfr maximum (730 nm)/Pr maximum (666 nm) ratio of 0.57–0.59, in agreement with previously published values (Vierstra & Quail, 1983a). All large phytochrome A used had a Pfr maximum (724–725 nm)/Pr maximum (668 nm) ratio in agreement with accepted values [0.43–0.48; Vierstra and Quail (1983b)]. The molecular masses of large and intact preparations were confirmed to be 114–118 and 124 kDa, respectively, using SDS–PAGE.

*Circular Dichroism (CD).* CD spectra were taken on a Jasco J600 spectropolarimeter. Peptide and protein concentrations of 0.1 mg/mL (approximately $8.5 \times 10^{-4}$ M residue concentration) were used for all samples (except the 54-mer N-terminus) with and without SDS. Concentration determination was by careful measurement of dry weight except for the 54-mer N-terminus, where amino acid analysis was used to verify concentration determination by dry weight. The method of Manavalan and Johnson (1987) was used to calculate the structural composition of proteins with and without SDS. No convergence problems were encountered using data from 184 to 240 nm. However, this method was not used for the peptide structure determination, as relatively large errors were encountered. For example, peptone, which consists of small randomly coiled peptides (see discussion below) was calculated to have almost as much $\beta$-sheet (35%) as random coil (37%). This may be due to the low molar ellipticity of smaller peptides compared to proteins, since proteins are used as the basis set in the Manavalan and Johnson (1987) calculations. The Chen et al. (1978) method of $\alpha$-helix determination was used for the peptide spectra. This method affords a reasonable determination of $\alpha$-helix composition only. The numbers obtained are thus useful when helical compositions derived from other methods, such as the Manavalan and Johnson (1987) procedure, are compared.

*Absorbance Spectral Measurements.* A Shimadzu UV-265 spectrophotometer was used to record all spectra. Spectra were smoothed using a window of 5 nm. Aliquots of phytochrome A solution were pipeted into separate containers, and equal volumes of buffer or saturated (25 ± 1 °C) peptide solution were added to the phytochrome A. The 54-mer peptide concentrations varied from 9.0 (50% dilution of saturated) to 12.5 $\mu$M (30% dilution of saturated). Photoconversion of phytochrome A was carried out using a Fiber-Lite series 180 high-intensity illuminator from Dolan-Jenner Industries, Inc. (Woburn, MA) for 60 s. Red (660 nm) and far-red (730 nm) interference filters from The Optometrics Corp. (Ayer, MA) were used for wavelength selection. These filters have a half-bandwidth of 10 ± 2 nm and a blocking range of X-ray to 1200 nm.

For determination of binding constants and comparison of the native and synthetic peptide spectral effects, it was important to determine accurately the relative concentrations of intact and large phytochrome A. Phytochrome A concentrations were adjusted with respect to each other using the extinction coefficients of the Pr form. These coefficients are equivalent for intact and large phytochrome A at the respective maximum of each protein spectra (Vierstra & Quail, 1982). This is consistent with the fact that there are relatively minor changes in the Pr spectra compared to the Pfr spectra, even after extensive proteolytic degradation of phytochrome A (Jones & Quail, 1989).

*Mean Hydrophobic Moment ($\langle\mu\rangle$) Calculations.* $\langle\mu\rangle$ values were calculated according to Eisenberg et al. (1982) using the following equation:

$$\langle\mu\rangle = \{(\sum_{n=1}^{N} H_n \sin(\delta n))^2 + (\sum_{n=1}^{N} H_n \cos(\delta n))^2\}^{1/2}/N$$

where $N$ is a given window and $n$ is a specific residue within that window. $H_n$ is the hydrophobic value assigned to residue $n$, and $\delta$ is the angle between side chains of adjacent residues. Hydrophobic values of Eisenberg et al. (1982) were assigned and a window of 11 residues was used for all calculations. $\delta$ was taken to be 100° for $\alpha$-helices and 180° for $\beta$-sheets.

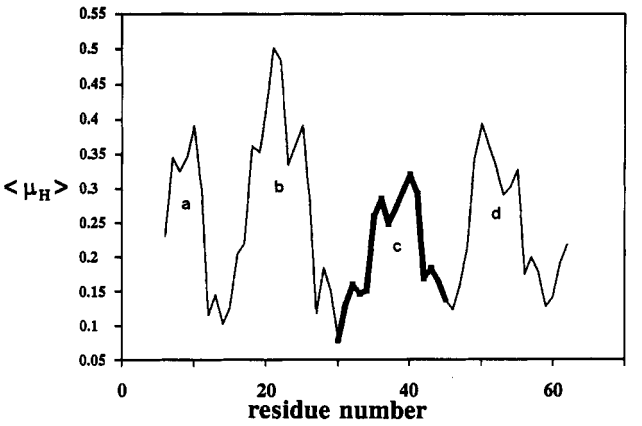


FIGURE 1: Average $\langle\mu_H\rangle$ diagram of the first 63 residues of *Avena*, *Cucurbita*, and *Pisum* phytochrome A's. Peaks are labeled alphabetically from the N-terminus to the C-terminus. $\langle\mu_H\rangle$ values were calculated as described in Materials and Methods. The conserved region determined by sequence identity is marked by the thicker line. Homology analysis of this sequence also indicates that this region is most highly conserved (Parker et al., 1990).

## RESULTS

*(a) Mean Helical Hydrophobic Moment ($\langle\mu_H\rangle$) Analysis of the Phytochrome A N-Terminal Chain.* The individual $\langle\mu_H\rangle$ diagrams for the N-terminal chains of nine sequenced phytochromes have previously been published (Parker et al., 1991). The consensus $\langle\mu_H\rangle$ diagram for the N-terminal region (63 residues) of *Avena*, *Cucurbita*, and *Pisum* phytochrome A's is shown in Figure 1. Four distinct peaks, labeled a–d in the diagram, are present. The approximate locations of the four peaks are from residues (a) 4–11, (b) 16–28, (c) 33–42, and (d) 47–54 (numbers vary slightly between sequences). In the three other type I or "etiolated" phytochrome (phytochrome A) sequences, there are differences in the region containing the first two peaks (peaks a and b, approximately residues 1–28). The *Maize* and *Oryza* sequences yield three narrow peaks in this region while the *Arabadopsis* PHYA sequence yields one large peak in this area. The most highly conserved region corresponds to peak c in Figure 1.

*(b) Amphiphilic Folding Potential Probed by SDS Micelle Interaction.* The CD spectra of two N-terminal peptides and two control peptides with and without SDS are shown in Figure 2. The 54-mer N-terminal segment (residues 1–54, *Avena* phytochrome A; Figure 2a) shows considerable interaction with SDS at an SDS concentration above the cmc. There was roughly an 83% increase in $\alpha$-helix (from 21.6% to 39.5%) judged by the method of Chen et al. (1974) using the ellipticity at 222 nm. The increase in ellipticity centered around 195 nm (from 190 to 200 nm) as well as the broad decrease in ellipticity from 205 to 235 nm is indicative of helix formation.

Residues 1–18 of *Avena* phytochrome A did not show the appreciable spectral change expected of helix or sheet formation (Figure 2b) upon interaction with SDS micelles. Although a difference in ellipticity of the random coil peak is evident (See Figure 2d for the coil spectra.), little change was observed above 215 nm.

A peptide not related to the N-terminal region of phytochrome A and having a high hydrophobic moment was used as a positive control. The 16-mer used (residues 1090–1104 of *Avena* phytochrome A, with an additional C-terminal cysteine) has high $\langle\mu_H\rangle$'s compared to other amphiphilic regions in a variety of proteins (Parker & Song, 1990). All five $\langle\mu_H\rangle$ values for the sequence are above 0.55 and have an average of 0.63. These values are the highest of the entire phytochrome A sequence (1128 residues), using the calculation

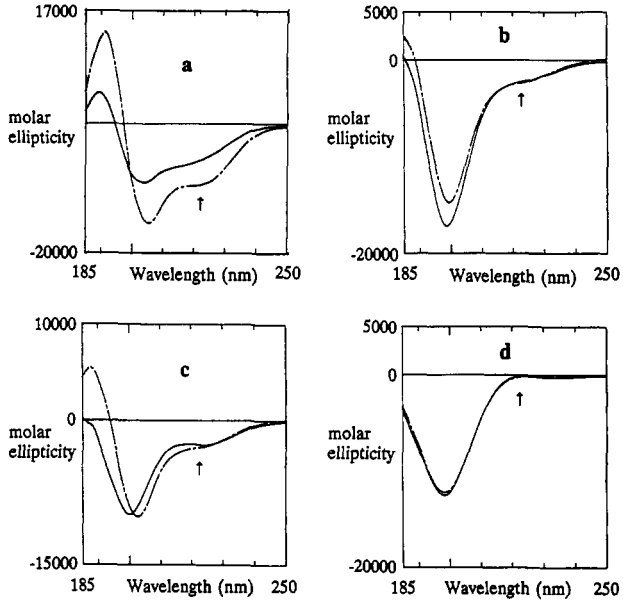


FIGURE 2: CD spectra of four peptides with (– · –) and without (—) 40 mM SDS. Arrows indicate 222 nm. All spectra were recorded in 10 mM sodium phosphate, pH 7.0. The units of ellipticity are in deg cm$^2$ dmol$^{-1}$. The peptides used were as follows: (a) N-terminal 54-mer peptide, (b) N-terminal 18-mer peptide, (c) C-terminal 16-mer peptide, and (d) peptone.

scheme of Parker and Song (1990). Interestingly, the CD spectra of the C-terminal peptide did not show typical changes associated with helix formation upon SDS micelle interaction (Figure 2c). The dramatic increase in ellipticity below 202 nm and the decrease in ellipticity from 202 to 222 nm are representative of ordered structure formation (sheet and/or helix). However, the lack of change at 222 nm rules out helix formation as the only process involved. This indicates that $\beta$-sheet may be involved in the SDS micelle interaction. A mean sheet hydrophobic moment ($\langle\mu_\beta\rangle$) analysis revealed two regions of possible amphiphilic $\beta$-strand formation. One region contained four consecutive $\langle\mu_\beta\rangle$'s greater than 0.55 (average of 0.66), and the second contained four consecutive $\langle\mu_\beta\rangle$'s greater than 0.75 (average of 0.90). Using the statistical approach of Parker and Song (1990), two $\langle\mu_\beta\rangle$ strings of this magnitude would be expected to occur less than once every $10^7$ residues.

Results from a negative control using nonamphiphilic (highly digested and hydrophilic) peptides are shown in Figure 2d. The single negative peak centered around 198 nm shows no change upon addition of 40 mM SDS. No evidence of either $\beta$-sheet or $\alpha$-helix is present in either the peptone or the 40 mM SDS + peptone spectra (Figure 2d).

Two intact proteins with markedly different amphiphilic properties were also studied with and without SDS. We have previously used hemoglobin as a control for amphiphilic $\alpha$-helical formation in SDS (Parker & Song, 1992), since it already has all of its amphiphilic regions in an $\alpha$-helical form. Figure 3A shows the change in the CD spectrum upon interaction of human hemoglobin with SDS micelles as measured by CD. There is a decrease in ellipticity from ~193 to 210 nm. The ellipticity increases (decrease in negative ellipticity in the original spectra) from approximately 210 to 235 nm. This is typical for a helix to coil transition. Note that this is roughly the inverse of the 54-mer N-terminal response to 40 mM SDS (Figure 2a). Analysis of the spectra by the method of Manavalan and Johnson (1987) indicated a 6% loss of $\alpha$-helical structure upon interaction with SDS micelles (Table I). Thus, ~91% of the helical structure in

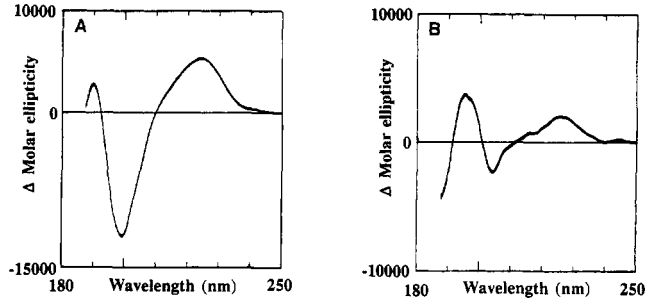


FIGURE 3: Difference (Δ) CD spectra of (A) hemoglobin and (B) papain. Both Δ spectra are calculated by subtracting the native protein spectrum from the spectrum in the presence of 40 mM SDS [(protein + SDS) – protein]. Sodium phosphate, 10 mM, pH 7.0, was used as the buffer in all solutions.

Table I: Percent $\alpha$-Helix, Antiparallel $\beta$-Sheet, Parallel $\beta$-Sheet, $\beta$-Turn, and Aperiodic Structure[a]

| protein | $\alpha$-helix | A[b] $\beta$-sheet | P[b] $\beta$-sheet | $\beta$-turn | random coil |
|---|---|---|---|---|---|
| hemoglobin | 69 | 3 | –1 | 22 | 6 |
| hemoglobin + SDS | 63 | 0 | 1 | 23 | 15 |
| papain | 24 | 16 | 4 | 17 | 41 |
| papain + SDS | 23 | 19 | 4 | 20 | 34 |

[a] Calculated from the CD spectra used in Figure 3 according to the method of Manavalan and Johnson (1987). Ellipticity from 184 to 240 nm at 1-nm intervals was used in the calculations. [b] A, antiparallel; P, parallel.

hemoglobin remains intact, while the rest is converted to random coil.

The change in CD signal upon interaction of papain with SDS micelles is shown in Figure 3B. Unlike hemoglobin, papain clearly shows a tendency to form ordered structure in the presence of SDS micelles. The increase in ellipticity from 192 to 202 nm and the decrease in ellipticity (increase in negative ellipticity in the original spectra) from 202 to ~215 nm both indicate the formation of ordered structure (sheet and/or helix). Note that this is basically the same response to 40 mM SDS exhibited by the amphiphilic C-terminal peptide described above. The Manavalan and Johnson (1987) analysis of the spectra indicates that there is a significant increase in $\beta$-sheet and turn at the expense of coil structures (Table I). This apparently takes place in the absence of appreciable change in helical content (Table I).

(*c*) *Spectral Change upon N-Terminal Loss.* The difference (Δ) absorbance spectrum of Pfr(intact) – Pfr(large) is shown in Figure 4a. There is a broad absorbance change dependent on loss of the N-terminal region with a maximum at 737 nm. The spectral difference between large and intact Pr phytochrome A is not as pronounced as the Pfr difference [Vierstra and Quail (1983b); Figure 4a]. The intact Pr form has more absorbance from about 580 to 667 nm with a maximum difference at 643 nm. The Δ absorbance minimum of the Pr(intact) – Pr(large) is at 679 nm and is 50% greater in magnitude than the ΔPr maximum (645 nm). The difference spectrum of the Pr molecule (Figure 4a) is due to a ~2-nm red shift of the Pr spectrum upon loss of the N-terminal region (Vierstra & Quail, 1983b).

The [Pfr(intact) – Pr(intact)] – [Pfr(large) – Pr(large)] ΔΔ absorbance spectrum is shown in Figure 4b. This spectrum indicates the overall effect of the loss of the N-terminus on the phytochrome A spectra, including both the Pr and the Pfr forms.

(*d*) *Spectral Change upon Addition of N-Terminal Peptide to Large Phytochrome A.* The ΔΔ absorbance spectra of (Pfr

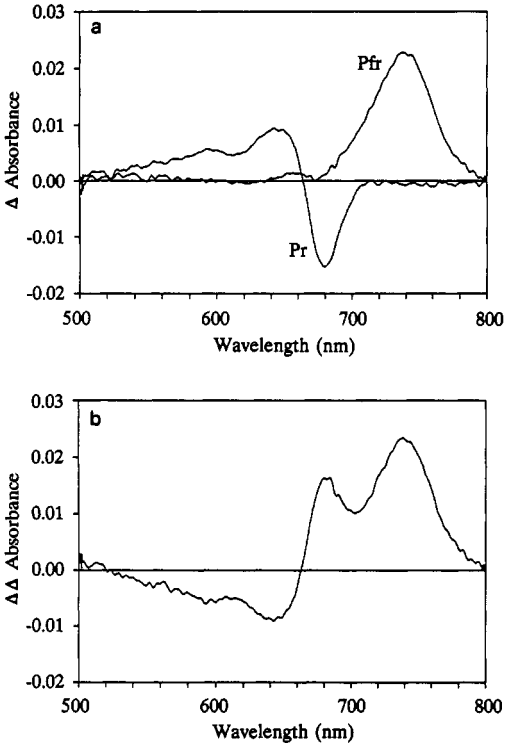


FIGURE 4: (a) Δ absorbance spectra showing both the Pfr(intact) – Pfr(large) and Pr(intact) – Pr(large) spectra from 500 to 800 nm. (b) The ΔΔ absorbance spectra of intact vs large phytochrome A, [Pfr(intact) – Pr(intact)] – [Pfr(large) – Pr(large)]. A phytochrome A concentration of 16 μM was used. A small concentration adjustment between the large and intact samples was made by assuming that the absorption maximum of the Pr form is the same in magnitude for both intact and large phytochrome A (Vierstra & Quail, 1983b). Spectra were taken in 20 mM sodium phosphate, pH 7.8, and 1 mM EDTA.

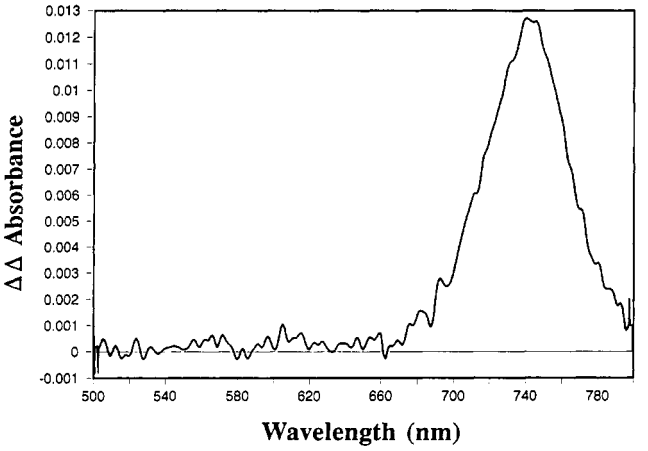


FIGURE 5: ΔΔ absorbance spectrum of large phytochrome A with and without 54-mer peptide, (Pfr – Pr; 54-mer peptide present) – (Pfr – Pr). A phytochrome A concentration of 2.4 μM and a peptide concentration of 9.0 μM were used.

– Pr; 9 μM 54-mer peptide present) – (Pfr – Pr) using large phytochrome A is shown in Figure 5. This spectrum is effected by both the Pfr and the Pr peptide interactions. The ΔΔ absorbance spectrum comparing large and intact phytochrome (Figure 4b) is significantly affected by change in the Pr spectra. On the other hand, there is no detectable influence of the Pr spectra on the ΔΔ absorbance spectrum using the 54-mer (Figure 5). The ΔΔ absorbance spectrum using the 54-mer (Figure 5) is essentially superimposable on the Pfr(intact) – Pfr(large) difference spectrum (Figure 4a). Both difference spectra show difference maxima near 740 nm.

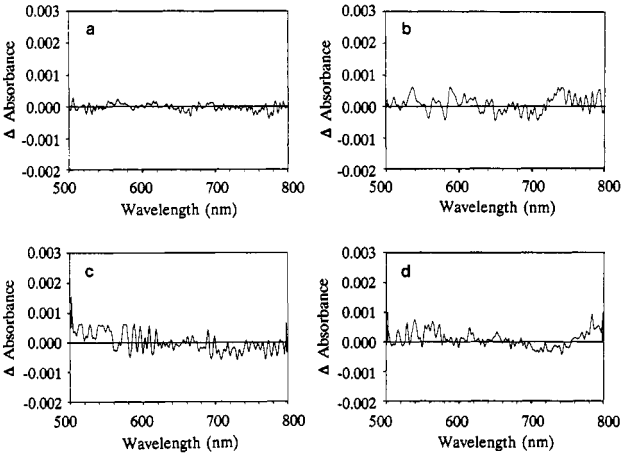


FIGURE 6: Δ absorbance spectra of (a) [Pr(large) + 54-mer peptide] – Pr(large), (b) [Pfr(large) + C-terminal peptide] – Pfr(large), (c) [Pfr(large) + 18-mer N-terminal peptide] – Pfr(large), and (d) [Pfr-(intact) + 54-mer peptide] – Pfr(intact). A phytochrome A concentration of 0.62 μM was used for the interaction of the 54-mer with phytochrome A. A 54-mer peptide concentration of 12.5 μM was also used. For control experiments (spectra b–d), higher phytochrome A (1.4 μM) and significantly higher peptide (0.5 mg/mL) concentrations were used. Sodium phosphate 10 mM, (pH 7.8)/0.5 mM EDTA was used as a buffer in all solutions.

Assuming that the large Pfr–peptide complex is spectrally identical to intact phytochrome A, a dissociation constant ($K_D$) of $2.1 \times 10^{-5}$ M (25 °C) can be calculated from the amplitude values of the difference spectra. Concentrations of both large and intact phytochrome A were determined by the Pr extinction coefficient, which is equivalent for both proteins (Vierstra & Quail, 1982). The $K_D$ corresponds to a $\Delta G^0$ of –26.7 kJ/mol or –6.37 kcal/mol for the complex formation, using $\Delta G^0 = -RT \ln K_D$.

The (Pr + 12.5 μM 54-mer peptide) – Pr spectrum using large phytochrome A is shown in Figure 6a. No interaction is evident, although if any interaction did exist, it may not be visible using these experimental concentrations.

The Δ absorbance spectrum of (Pfr + 270 μM C-terminal peptide) – Pfr using large phytochrome A is shown in Figure 6b. There are no peaks evident above the noise level in the spectrum. The same experiment performed with 270 μM 18-mer N-terminal peptide produced the same result (Figure 6c), as did the use of 0.5 mg/mL peptone (spectra not shown). Also, addition of the 54-mer N-terminus to intact 124-kDa phytochrome A as Pfr produced no detectable spectral change (Figure 6d).

It is worthy of note that the interaction of large phytochrome A with peptide preparations which were not chromatographically purified yielded a slightly different result from that seen in Figure 5. In addition to the spectral change seen in Figure 5, there was an additional increase in absorbance from 690 to 720 nm and a decrease in absorbance from 660 to 690. This is indicative of a spectral shift centered around 690 nm. This may be due to sulfhydryl scavengers or protecting groups which were present in the unpurified peptide preparation.

## DISCUSSION

N-terminal α-helical folding of *Avena* phytochrome A upon Pr to Pfr photoconversion has been well documented in the literature (Chai et al., 1987a; Vierstra et al., 1987; Sommer & Song, 1990). Similar α-helical folding has also been observed in *Pisum* phytochrome A (unpublished data by L. Deforce, S. Tokutomi, and P.-S. Song, 1992). The inhibition of this folding by antibody binding to the N-terminal chain

(Chai et al., 1987a), the effect on the change imposed by different buffer systems (Sommer & Song, 1990), and the CD difference spectrum (Parker et al., 1991) all indicate that there is a conformational change in the peptide backbone rather than a change in the CD spectrum induced by chromophore/protein interactions.

A model of the phytochrome A holoprotein has been developed which includes several properties associated with this helical folding. The phytochrome A chromophore is known to reside in a hydrophobic pocket (Hahn & Song, 1981). Both bleaching and chelation studies demonstrate that the chromophore and this hydrophobic pocket become more exposed to solvent upon conversion of Pr to the Pfr form (Hahn et al., 1984; Sommer & Song, 1990). The degree of Pfr chromophore exposure is considerably less in intact phytochrome A as compared to large phytochrome A (Hahn et al., 1984). This indicates that the N-terminal region is adjacent to and shielding the Pfr chromophore/chromophore pocket from solvent. The bathochromic effect on the Pfr spectrum of the N-terminal region (Vierstra & Quail, 1983b) was further indication that the peptide is interacting specifically with the Pfr chromophore. Detailed proteolysis maps of the N-terminal region (Grimm et al., 1988) using various enzymes show that the Pr N-terminus is exposed at several sites spread over the entire region (Arg-20, Asn-32, Lys-46, Glu-49, Arg-52, Glu-63, Lys-64, and Tyr-68). These are all early cleavage sites of Pr, but only the Glu-63, Lys-64, and Tyr-68 cleavage sites are found in Pfr (Grimm et al., 1988).

The previously proposed models of the Pr and Pfr phytochrome A conformations included the above points. They also suggested the possibility of induced amphiphilic $\alpha$-helical folding upon conversion of Pr to Pfr due to exposure of a hydrophobic chromophore/chromophore pocket. This pocket or hydrophobic surface would then stabilize N-terminal $\alpha$-helices by binding or interacting with the hydrophobic surfaces of N-terminal amphiphilic helices.

The $\langle\mu_H\rangle$ diagram (Figure 1) of the phytochrome A N-terminal chain demonstrates that there is amphiphilic helical potential in that region. Qualitatively, the magnitudes of that potential as calculated according to Eisenberg et al. (1982) are equivalent to values seen on the shorter helices (7–12 residues) of myoglobin or other proteins containing a distinct hydrophobic pocket. Higher values around 0.5 or 0.6 are commonly seen in longer helices of these proteins. Also, interactions between the peptide and charged or polar groups on prosthetic groups tend to lower the calculated amphiphilic potential (Parker & Song, 1990). This may be the case in the N-terminal interaction with the chromophore/chromophore pocket, given the presence of several charged and polar groups on the chromophore. Perhaps the region containing peak c in Figure 1 (residues 33–42) is the best candidate for this chromophore interactive site, since it has both the smallest $\langle\mu_H\rangle$ values and the most highly conserved sequence. Clearly, the presence of this helical potential does not mean that the peptide must assume $\alpha$-helix in either the Pr or Pfr form, but it does demonstrate that the potential exists.

The SDS micelle interaction study using both peptides (Figure 2) and proteins (Figure 3) clearly shows that the phytochrome A 54-mer N-terminal chain has amphiphilic helical potential under the conditions used. Control peptides (peptone and the phytochrome A C-terminal peptide) did not show any tendency to form an $\alpha$-helix under the conditions used, although the C-terminal peptide did form a $\beta$-sheet. This C-terminal control demonstrates that, under these conditions, helical amphiphilic potential alone is not sufficient to ensure helix formation in an amphiphilic environment. There must also be some tendency of the particular sequence involved to assume a helical conformation. The 83% increase in helix found by the Chen et al. (1974) CD analysis of the 54-mer N-terminal chain indicates that the N-terminus does indeed have a significant tendency to form amphiphilic $\alpha$-helices. Perhaps the first 33% of the peptide is not involved in this helical folding under these conditions, since this region alone shows no sign of helical folding in the presence of SDS (Figure 2b). If this is the case, then residues Ala-19 through Gly-54 of the N-terminus would undergo a 32–59% helix transition upon interaction with SDS micelles. In this interaction, the formation of helices is induced by the presence of hydrophobic areas inside micelles. The hydrophobic chromophore/chromophore pocket could presumably behave in this same manner in the Pfr form but not in the Pr form, where this pocket is not exposed (Hahn & Song, 1981; Hahn et al., 1984; Thümmler et al., 1985; Farrens et al., 1989).

Two indications that amphiphilic helical formation may be the mode of $\alpha$-helix formation during Pr to Pfr phototransformation are (i) amphiphilic helical potential is present in the phytochrome A N-terminal chain (Figure 1) and (ii) the N-terminal chain forms helical structures in an amphiphilic environment (SDS micelles; Figure 2). This putative amphiphilic $\alpha$-helical folding, suggested by the current phytochrome A model, is also consistent with the observation that the difference in helical content between Pr and Pfr was not observable by infrared (IR) spectroscopy (Siebert et al., 1990). On the basis of the amphiphilicity of the N-terminal region (Figures 1 and 2), the largely exposed Pr N-terminal chain would be expected to form an $\alpha$-helix when in an amphiphilic environment. Thus, under amphiphilic conditions [such as the films used in IR measurements: amphiphilic or surfactant peptides form an $\alpha$-helix at air/water interfaces (DeGrado & Lear, 1985; Minakata et al., 1989)], helical formation in the exposed N-terminal chain of the Pr form of phytochrome A should diminish the differences in secondary structure between the Pr and Pfr forms of phytochrome A. The alteration of phytochrome A structure by air/water amphiphilic interfaces is further supported by the fact that phytochrome A forms surface layers which have been studied on a Langmuir film balance (Kim et al., 1989).

The behavior of the 18-mer N-terminus in the presence of 40 mM SDS differs significantly from the 54-mer behavior (Figure 2). Ten out of the first 17 residues of *Avena* phytochrome A are serine. This amino acid is commonly known to be a "helix-breaking" rather than a helix-forming residue (Chou & Fasman, 1978). This seems to be consistent with the lack of helix formation under the conditions we employed both with and without SDS (Figure 2). No further increase in $\alpha$-helix was seen by CD in this peptide even at 4 $\pm$ 2 °C in the absence of SDS. This indicates that there is no random coil to helix equilibrium present, as helix is favored at low temperatures if any equilibrium does exists. On the other hand, recent experimental evidence clearly demonstrates that, for some reason, two consecutive serines do not behave in a helix-breaking fashion as does a single serine (O'Neil & DeGrado, 1990). All of the serines in the first 17 residues of phytochrome A occur in groups of 2 or more. Thus, it is not clear whether or not this far N-terminal region (residues 1–17) is able to undergo induced amphiphilic helix formation in the native molecule under native conditions.

To further complicate the role of this far-N-terminal serine-rich region, it is known that this area is a phosphorylation site in Pr, but not in Pfr (Wong et al., 1986). Phosphate analysis

of purified *Avena* phytochrome A has yielded a phosphate to phytochrome A ratio of 1:1 (Hunt & Pratt, 1980). However, recent evidence indicates that there are two in vivo phosphorylation sites in *Avena* phytochrome A (McMichael, 1991). Both sites are phosphorylated in roughly equal amounts, judging by phosphopeptide production after enzymatic digestion (McMichael, 1991). Thus, the phosphorylation level of the N-terminal region of phytochrome A in vivo may be ~50%, but more work is needed to verify this number. The effect of phosphorylation on the N-terminus may cause a dramatic increase in helical amphiphilic character, although this is not known. The phosphorylation of the helical amphiphilic phytochrome A N-terminus may be analogous to the phosphorylation of endogenous protein phospholamban in muscle tissue (Vorherr et al., 1992). The N-terminal portion of this molecule is described as an amphiphilic $\alpha$-helix which is phosphorylated to stimulate ATPase activity (Movsesian et al., 1984; Le Peuch et al., 1979). This N-terminal phospholamban peptide is the actual receptor-binding domain of phospholambin, and it is structurally similar to $Ca^{2+}$ pump effectors (Chiesi et al., 1991).

Due to spectral changes in large phytochrome A upon addition of synthetic 54-mer peptide (Figure 5), it is clear that a complex between the two is being formed in the Pfr form, although this is not the case with the Pr form (Figure 6a). The similarity between the spectral changes caused by loss of the native N-terminus (Figure 4a) and addition of the synthetic N-terminus (Figure 5) indicates that the interaction between synthetic peptide and large phytochrome A is nativelike. Addition of the 18-mer N-terminal fragment (Figure 6c), the C-terminal fragment (Figure 6b), and peptone (spectra not shown) produced no detectable spectral change in the large Pfr spectra. Addition of the synthetic 54-mer N-terminus to intact phytochrome A produced no spectral change in either Pr (spectra not shown) or Pfr (Figure 6d). These controls indicate that the interaction of the 54-mer peptide with large Pfr is specific for the sequence in the N-terminal region. Additionally, photocycling of large phytochrome A from Pr to Pfr and back to Pr in the presence of peptide still yielded no detectable spectral change in the Pr molecule, although any transient change may not have been detected (spectra not shown). The possibility that the 54-mer N-terminus peptide does form a complex with intact phytochrome A and/or large Pr, but does not affect the spectra, has not been ruled out.

The $\Delta G^0$ of –26.7 kJ/mol or –6.37 kcal/mol determined for the binding of the N-terminal peptide to large phytochrome A is a relatively large amount of free energy and is comparable to the differences between native and denatured states of proteins. This large difference may be due to (i) hydrogen bonding between the N-terminal peptide and the Pfr chromophore and (ii) a significant interaction of hydrophobic parts of the free peptide with solvent, which is expected since the peptide does contain amphiphilic regions (Figure 1) that are unordered in solution (Figure 2). Significant interaction of hydrophobic areas of the free peptide with solvent is also suggested by the poor solubility of the peptide. Calculation of the free energy of solvation using $\Delta G^0 = -RT \ln K$ ($K$ = 18 $\mu$M, determined by amino acid analysis) yields a solvation energy of 27.1 kJ/mol or 6.48 kcal/mol (25 °C). This is approximately the same amount of energy involved in binding of the peptide to large phytochrome A.

In conclusion, analysis of the 6-kDa N-terminal region of phytochrome A based on the primary sequence indicates that the potential to form amphiphilic $\alpha$-helix exists. Further, SDS micelle interaction studies of a synthetic phytochrome A N-terminal peptide show that the sequence does form amphiphilic helices in certain amphiphilic environments. This is consistent with the idea that the N-terminal chain of phytochrome A interacts with a hydrophobic chromophore/chromophore pocket in an amphiphilic $\alpha$-helical manner. In addition, this peptide actually interacts with the N-terminal chain truncated phytochrome A in the Pfr form lacking the 6-kDa N-terminal region, as demonstrated spectrally. This observation may provide us with a useful tool to probe N-terminal/chromophore interactions as well as involvement of this N-terminal region in the mechanism and functional implications of photoinduced conformational changes in phytochrome A.

## ACKNOWLEDGMENT

We thank Bruce Baggenstoss and Theodore Mahowald at the University of Nebraska Medical Center Protein Structure Core Facility for the use of their facilities and expertise. We also thank Renke Dai for help in peptide purification and Susanne Meza-Keuthen for careful reading of the manuscript.

## REFERENCES

Chai, Y.-G., Song, P.-S., Cordonnier, M.-M., & Pratt, L. H. (1987a) *Biochemistry 26*, 4947–4952.
Chai, Y.-G., Singh, B. R., Song, P.-S., Lee, J., & Robinson, G. W. (1987b) *Anal. Biochem. 163*, 322–330.
Chen, Y.-H., Yang, J. T., & Chau, K. H. (1974) *Biochemistry 13*, 3350–3359.
Cherry, J. R., Hondred, D., Keller, J. M., Hershey, H. P., & Vierstra, R. D. (1991) in *Phytochrome Properties and Biological Action* (Thomas, B., & Johnson, C., Eds.) NATO ASI Series H50, pp 113–127, Springer-Verlag, Berlin.
Cherry, J. R., Hondred, D., Walker, J. M., & Vierstra, R. D. (1992) *Proc. Natl. Acad. Sci. U.S.A. 89*, 5039–5043.
Chiesi, M., Vorherr, T., Falchetto, R., Waelchli, C., & Carafoli, E. (1991) *Biochemistry 30*, 7978–7983.
Chou, P. Y., & Fasman, G. D. (1978) *Annu. Rev. Biochem. 47*, 251–276.
Cordonnier, M. M., Greppin, H., & Pratt, L. H. (1985) *Biochemistry 24*, 3246–3253.
DeGrado, W. F., & Lear, J. D. (1985) *J. Am. Chem. Soc. 107*, 7684–7689.
Eisenberg, D., Weiss, R. M., & Terwillinger, T. C. (1982) *Nature 299*, 371–374.
Farrens, D., Song, P.-S., Rüdiger, W., & Eilfeld, P. (1989) *J. Plant Physiol. 134*, 269–275.
Grimm, R., Lottspeich, F., Schneider, H. A. W., & Rüdiger, W. (1986) *Z. Naturforsch. 41C*, 993–1000.
Grimm, R., Eckerskorn, C., Lottspeich, F., Zenger, C., & Rüdiger, W. (1988) *Planta 174*, 396–401.
Hahn, T.-R., & Song, P.-S. (1981) *Biochemistry 20*, 2602–2609.
Hahn, T.-R., Song, P.-S., Quail, P. H., & Vierstra, R. D. (1984) *Plant Physiol. 74*, 755–758.
Hunt, R. E., & Pratt, L. H. (1980) *Biochemistry 19*, 390–394.
Jones, A. M., & Quail, P. H. (1989) *Planta 178*, 147–156.
Jones, A. M., Vierstra, R. D., Danials, S. M., & Quail, P. H. (1985) *Planta 164*, 501–506.
Kim, J.-H., Cotton, T. M., Uphaus, R. A., & Song, P.-S. (1989) 4th International Conference on Langmuir–Blodgett Films, Tsukuba, Japan, abstract.
Lark, L. R., Berzofsky, J. A., & Gierasch, L. M. (1989) *Pept. Res. 2*, 314–321.
Lauterwein, J., Bösch, C., Brown, L. R., & Wüthrich, K. (1979) *Biochim. Biophys. Acta 556*, 244–264.
Le Peuch, C. J., Haiech, J., & Damaille, J. G. (1979) *Biochemistry 18*, 5150–5157.
Manavalan, P., & Johnson, W. C., Jr. (1987) *Anal. Biochem. 167*, 76–85.

McMichael, R. W. (1991) Ph.D. Dissertation, University of California, Davis.
Minakata, H., Taylor, J. W., Walker, M. W., Miller, R. J., & Kaiser, E. T. (1989) *J. Biol. Chem. 264*, 7907–7913.
Movsesian, M. A., Nishikawa, M., & Andelstein, R. S. (1984) *J. Biol. Chem. 259*, 8029–8032.
O'Neil, K. T., & DeGrado, W. F. (1990) *Science 250*, 646–651.
Parker, W., & Song, P.-S. (1990) *J. Biol. Chem. 265*, 17568–17575.
Parker, W., & Song, P.-S. (1992) *Biophys. J. 61*, 1435–1439.
Parker, W., Romanowski, M., & Song, P.-S. (1991) in *Phytochrome Properties and Biological Action* (Thomas, B., & Johnson, C., Eds.) NATO ASI Series H50, pp 85–112. Springer-Verlag, Berlin.
Pasta, P., Carrea, G., Longhi, R., & Zetta, L. (1990) *Biochim. Biophys. Acta 1039*, 1–4.
Siebert, F., Grimm, R., Rüdiger, W., Schmidt, G., & Scheer, H. (1990) *Eur. J. Biochem. 194*, 921–928.
Sommer, D., & Song, P.-S. (1990) *Biochemistry 29*, 1943–1948.
Thümmler, F., Eifeld, P., Rüdiger, W., Moon, D.-K., & Song, P.-S. (1985) *Z. Naturforsch. 40C*, 215–218.
Tsikaris, V., Sakarellos-Daitsiotis, M., Panou-Pomonis, E., Sakarellos, C., & Marraud, M. (1989) *Int. J. Pept. Protein Res. 33*, 195–201.
Vierstra, R. D., & Quail, P. H. (1982) *Planta 156*, 158–165.
Vierstra, R. D., & Quail, P. H. (1983a) *Biochemistry 22*, 2498–2505.
Vierstra, R. D., & Quail, P. H. (1983b) *Plant Physiol. 72*, 264–267.
Vierstra, R. D., Quail, P. H., Hahn, T.-R., & Song, P.-S. (1987) *Photochem. Photobiol. 45*, 429–432.
Voherr, T., Chiesi, M., Schwaller, R., & Carafoli, E. (1992) *Biochemistry 31*, 371–376.
Wong, Y.-S., Cheng, H.-C., Walsh, D. A., & Lagarias, J. C. (1986) *J. Biol. Chem. 261*, 12089–12097.
Wu, C.-S. C., & Yang, J. T. (1981) *Mol. Cell. Biochem. 40*, 109–122.